RSC Advances

PAPER

View Article Online
View Journal | View Issue

Cite this: *RSC Adv.*, 2015, **5**, 53189

A new fluorescent chemosensor for highly selective and sensitive detection of inorganic phosphate (Pi) in aqueous solution and living cells†

Qingtao Meng,*[a] Yue Wang,[a] Ming Yang,[a] Run Zhang,*[b] Renjie Wang[c] and Zhiqiang Zhang[a]

Received 11th May 2015
Accepted 11th June 2015

DOI: 10.1039/c5ra08712k

www.rsc.org/advances

In this work, a new fluorescence chemosensor, **FP**-Fe^{3+} was developed for the detection of Pi in aqueous solution and living cells. The unique ligand, **FP** displayed a high affinity to Fe^{3+} ($K_a = 1.40 \times 10^6$ M^{-1}) in the presence of other competing cations, accompanied with a dramatic fluorescence quenching. The specific interaction of Pi and **FP**-Fe^{3+} ensemble led to the liberation of fluorophore, **FP**, and thus the fluorescence was recovered. The dose-dependent fluorescence enhancement of **FP**-Fe^{3+} showed a good linearity with a detection limit of 300 nM for Pi. The extraordinary performance of the present chemosensor, including high sensitivity, selectivity, and good biocompatibility enable the investigation of fluorescent response for Pi in living cells by confocal microscope. Quantitative monitoring of intracellular Pi was achieved by the flow cytometry analysis.

Introduction

The development of recognition and sensing systems for anions have received considerable attention in recent years due to their fundamental roles in biology and environmental systems.[1] Among various anions, the phosphate anion is ubiquitous in biological systems and it plays important roles in numerous biological and chemical processes, such as cellular signaling, membrane integrity, muscle function, bone mineralization, *etc.*[2] In live organisms, inorganic phosphate (Pi), including $H_2PO_4^-$, HPO_4^{2-}, and PO_4^{3-}, is essential in diverse cellular functions involving intermediary metabolism and energy transfer.[3] The abnormal level of Pi in body fluids, such as blood serum, urine, or saliva is causal to or can exacerbate irregular physiological functions. It is reported that the deficiency of Pi is involved in muscle weakness, impaired leukocyte function, and irregularity in bone mineralization. While the increased level of Pi has been implicated with abnormal renal function.[4] Therefore, considerable effort has been devoted to the development of novel fluorescence chemosensors for Pi detection, particularly in physiological conditions.[5]

Based on hydrogen bonding with amide, urea, and thiourea subunits, a number of chemosensors for Pi detection have been developed.[6] However, none of them meet the requirements for the biological applications, which are as follows: (1) be highly specific for Pi detection in aqueous, (2) be capable of penetration the cell membrane, (3) be non-toxic and display fluorescence changes upon the detection of Pi in live cells. A few examples of selective recognition sensors for Pi in aqueous have been reported in recent years,[5d–f,j,o] but only one can be employed in living system.[5o] Nevertheless, it would be desirable to shift the excitation wavelength towards the visible region to reduce the effects of excitation phototoxicity on the biological samples.[7]

Recently, the displacement approach using corresponding cation coordination complexes has been reported as the strategy to design of anions chemosensors.[8] In which the fluorophore–metal complex "ensemble" is nonfluorescent due to the metal-ion-induced fluorescence quenching. The addition of anions may release the fluorophores into the solution with revival of fluorescence.[9] Based on the displacement strategy, we have developed a series of luminescence chemosensors for the anions detection in aqueous solution and successfully demonstrated their application in biological and environmental samples.[10] In this work, considering the fluorescence quenching properties of Fe^{3+} ion due to its paramagnetic nature and the advantage of high Fe^{3+}–Pi affinity, we may reasonably expect to prepare a new fluorescence chemosensor for Pi detection in aqueous and living system based on displacement approach.

Herein, a unique ligand, **FP**, which shows selective fluorescence quenching by Fe^{3+} *via* forming a **FP**-Fe^{3+} complex was designed and facilely synthesized. In the presence of Pi, the

[a]*School of Chemical Engineering, University of Science and Technology Liaoning, Anshan, 114044, China. E-mail: qtmeng@ustl.edu.cn; Tel: +86-421-5928009*

[b]*Department of Chemistry and Biomolecular Sciences, Faculty of Science and Engineering, Macquarie University, Sydney, NSW, 2109, Australia. E-mail: run.zhang@mq.edu.au; Tel: +61 2 9850 1175*

[c]*School of Chemistry and Molecular Biosciences, The University of Queensland Brisbane, Queensland, Australia*

† Electronic supplementary information (ESI) available. See DOI: 10.1039/c5ra08712k

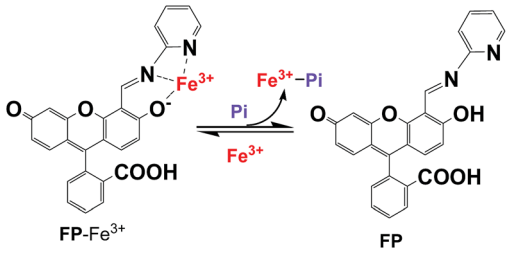

Scheme 1 The proposed mechanism for Pi detection by FP-Fe^{3+} ensemble.

detachment of Fe^{3+} ion on **FP**-Fe^{3+} complex led to a remarkable fluorescence enhancement (Scheme 1). The proposed mechanism of displacement approach was confirmed by the results of mass spectra studies. The **FP**-Fe^{3+} ensemble showed highly selective, sensitive, low cytotoxicity, widely available pH range towards Pi in HEPES buffer. By employing the confocal microscopy, we successfully demonstrated the application of the proposed chemosensor to monitor the Pi in living cells. Quantitative monitoring of intracellular Pi was achieved by the flow cytometry analysis.

Results and discussion

Design, synthesis and characterization of fluorescence chemosensor

Owning to its excellent photochemical and photophysical properties, such as long-wavelength absorption and emission, high fluorescence quantum yield and high stability against light,[11] fluorescein was chosen to be as the fluorophore in the present work. The unique ligand, **FP** was designed with a fluorescein as the signal unit and a 2-((pyridin-2-yl-imino)methyl) phenol moiety as the receptor to the Fe^{3+} ions. We envisioned that the fluorescence of **FP** could be effectively quenched due to the paramagnetic nature of Fe^{3+} ions,[12] and the decomplexing of Fe^{3+} in the presence of Pi could lead to a fluorescence restoration. Thus, the non-fluorescence **FP**-Fe^{3+} ensemble could be employed as the platform for Pi detection.

The unique ligand, **FP** was facilely synthesized by a one-step reaction of 4-fluoresceincarboxaldehyde with 2-aminopyridine in methanol (Scheme S1, ESI†). The structure of **FP** was confirmed by NMR, mass spectra and elemental analysis (Fig. S1–S3, ESI†). Both **FP** and **FP**-Fe^{3+} are stable in aqueous, which is confirmed by the results of fluorescent intensity measurements (Fig. S4, ESI†). The proposed displacement strategy for the Pi detection was further supported by the results of mass spectra studies. As shown in Fig. S3,† ESI-MS spectra showed a molecular-ion peak $[\mathbf{FP} + H^+]^+$ at m/z 437.2. When the Fe^{3+} ion was added into the solution of **FP**, the peak at m/z 538.4 is assignable to $[\mathbf{FP} - H^+ + Fe^{3+} + 2Cl^- + Na^+]^+$ species (Fig. S5, ESI†). This result confirmed that 1 : 1 stoichiometry complex between **FP** and Fe^{3+}. In the presence of Pi, ESI-MS spectra displayed a molecular-ion peak at m/z 437.2 again (Fig. S6, ESI†), indicating that the decomplexing of Fe^{3+} ion in the presence of Pi led to the liberation of fluorophore, **FP**.

Fluorescence emission spectrum studies of FP with various metal ions

The fluorescence response of **FP** towards various metal ions was evaluated in HEPES aqueous buffer (THF : H_2O = 3 : 7, 20 mM, pH = 7.4). The quenching rate (F_0/F) of the emission intensities at 515 nm of **FP** (10 μM) in the present of competitive cations were shown in Fig. 1. The addition of 3×10^{-4} M Fe^{3+} result in about 56-fold fluorescence quenching of **FP**, while a negligible response of the **FP** was observed with other metal ions, such as Hg^{2+}, Cd^{2+}, Pb^{2+}, Zn^{2+}, Ni^{2+}, Co^{2+}, Mn^{2+}, Cr^{3+}, Ag^+ and Ca^{2+}, Mg^{2+}, Ba^{2+}, Li^+, K^+, Na^+. Although 11.5-fold quenching were observed in the present of equal amounts of Cu^{2+}, the addition of 3×10^{-4} M Fe^{3+} to the above solution gave rise to a significant fluorescence quenching in accordance with the addition of equal equiv. of Fe^{3+} alone, indicating that specific response of **FP** to Fe^{3+} ions was not disturbed by other competitive cations.

To quantitatively evaluate the fluorescence quenching and the **FP**-Fe^{3+} binding, the fluorescence intensities of **FP** (10 μM) in the presence of different concentrations of Fe^{3+} were measured. As shown in Fig. 2, the fluorescence chemosensor **FP** displayed strong green fluorescence at 515 nm in HEPES aqueous buffer with pH 7.4. By the addition of 3×10^{-4} M of Fe^{3+}, the fluorescence intensity of **FP** (10 μM) was completely quenched (the quenching efficiency at 515 nm was 94%), which could be ascribed to the paramagnetic quenching effect of Fe^{3+} and/or ligand to metal charge transfer (LMCT).[13] Job's plot analysis confirmed that **FP**-Fe^{3+} ensemble was formed according to a 1 : 1 stoichiometry (Fig. S7, ESI†).[14] According to linear Benesi–Hildebrand expression, the fluorescence intensity $[1/(F_0 - F)]$ of **FP** at 515 nm varied as a function of $1/[Fe^{3+}]$ in a linear relationship (R^2 = 0.993), corroborated that Fe^{3+} and **FP** was complexed by a 1 : 1 stoichiometry (Fig. S8, ESI†).[15] The association constant of **FP** with Fe^{3+} in HEPES buffer was calculated to be 1.40×10^6 M^{-1}. The fluorescence changes ($\Delta F = F_0 - F$) *vs.* Fe^{3+} concentration displayed in Fig. S9.† The result revealed a good linearity of the common ΔF *vs.* $[Fe^{3+}]$ from 0 to 20 μM ($Y = 12.099X + 1.333$, $R^2 = 0.997$). The limit of detection was estimated to be

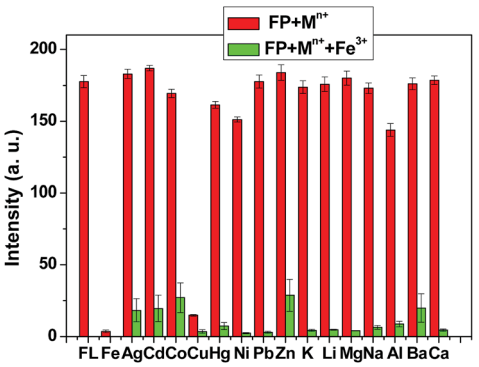

Fig. 1 Fluorescence responses of FP (10 μM) towards various cations in HEPES buffer (THF : H_2O = 3 : 7, 20 mM, pH = 7.4). The red bars represent the emission changes of FP in the presence of cations of interest (3×10^{-4} M). The green bars represent the changes of the emission that occurs upon the subsequent addition of 3×10^{-4} M of Fe^{3+} to the above solution. The intensities were recorded at 515 nm, excitation at 430 nm.

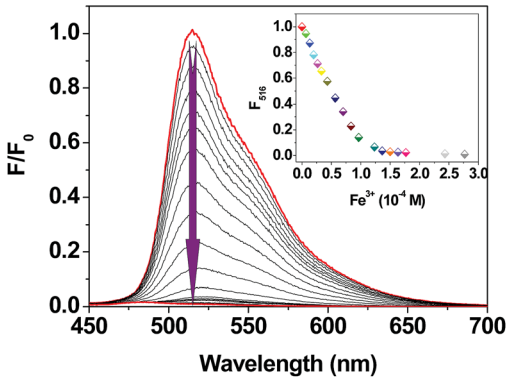

Fig. 2 Fluorescence spectra of **FP** (10 μM) in HEPES aqueous buffer (THF : H_2O = 3 : 7, 20 mM, pH = 7.4) in the presence of different amounts of Fe^{3+} (0–3.0 × 10^{-4} M). Insert: normalized fluorescence intensities of **FP** (10 μM) at 515 nm as a function of Fe^{3+} (0–3 × 10^{-4} M). Excitation was performed at 430 nm.

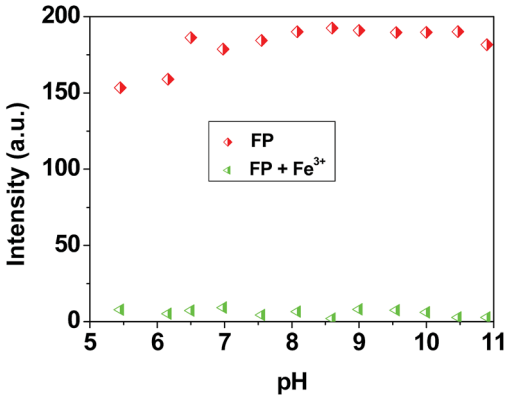

Fig. 4 Variations of fluorescence intensity at 515 nm of **FP** (10 μM) in THF–H_2O (3 : 7, v/v) with (bottom) and without (up) Fe^{3+} (0–3 × 10^{-4} M) as a function of pH. Excitation at 430 nm.

1.5 μM based on reported method defined by IUPAC,[16] which is below the maximum permissive level of Fe^{3+} in drinking water (5.37 μM) set by the U. S. Environmental Protection Agency.[17]

UV-vis absorption spectrum of **FP** in the presence of different concentrations of Fe^{3+} was further studied in HEPES buffer. As shown in Fig. 3, **FP** showed a typically fluorescein-based absorption maximum at 480 nm. When Fe^{3+} ion was gradually introduced into a solution of 10 μM **FP** in HEPES buffered, the intensity of absorption band was significantly increased, implicating the formation of a **FP**-Fe^{3+} ensembles.[18] In addition, the enhanced broad absorbance band ranging from 300 nm to 400 nm in the presence of increasing Fe^{3+} was also observed in the UV-vis titration, which could be assigned to the solvated Fe^{3+} species.[19] As shown in Fig. S10,† upon the addition of other physiological and environmental important ions, negligible changes of absorption spectra was observed, indicating the specific fluorescence quenching by Fe^{3+} ions.

Effect of pH

The effects of pH value on the fluorescence intensities of **FP** and **FP**-Fe^{3+} were evaluated. As shown in Fig. 4, **FP** exhibited strong and stable fluorescence emission at pH 6.0–11.0, and the **FP**-Fe^{3+} showed pH independent in the range of 5.5–11.0. The results indicated that the **FP** can be used as a chemosensor for Fe^{3+} detection and the **FP**-Fe^{3+} ensemble could work for the detection of Pi in the weakly acidic, neutral, and basic conditions.

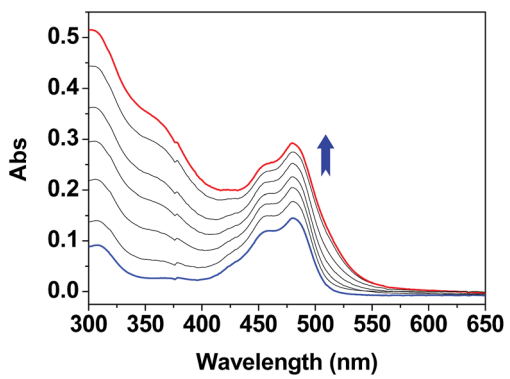

Fig. 3 UV-vis absorption spectra of **FP** (10 μM) in the presence of Fe^{3+} (0–3 × 10^{-4} M) in HEPES aqueous buffer (THF : H_2O = 3 : 7, 20 mM, pH = 7.4).

Fluorescence emission spectrum studies of FP-Fe^{3+} ensemble with various anions and nucleotides

By virtue of the extremely high Fe^{3+}–Pi affinity, **FP**-Fe^{3+} complex was expected to act as a potential chemosensor for Pi recognition *via* Fe^{3+} displacement approach. To evaluate the selectivity of **FP**-Fe^{3+} ensemble towards Pi, the fluorescence turn "ON" response of **FP**-Fe^{3+} to different biological important ions and adenosine phosphate series was investigated. As shown in Fig. 5, **FP**-Fe^{3+} showed negligible fluorescent response upon addition of diverse anions, such as Ac^-, Br^-, Cl^-, F^-, SCN^-, HSO_4^-, NO_2^-, OH^-, HCO_3^-, CO_3^{2-}, SO_4^{2-} and S^{2-}. Moreover, **FP**-Fe^{3+} displayed reasonable performance on discrimination Pi with other polyphosphate species, such as AMP, ADP, ATP and even pyrophosphate (PPi). The addition of these polyphosphate species into **FP**-Fe^{3+} solution in HEPES buffer led to much less increase in fluorescent intensity than Pi: *e.g.* AMP (1.45-fold), ADP (1.98-fold) and ATP (2.35-fold), PPi (3.7-fold). By contrast, the fluorescence of **FP**-Fe^{3+} was dramatically enhanced (9.6-fold) with the addition of 3 × 10^{-4} M Pi. In addition, to evaluate the utility of **FP**-Fe^{3+} as a fluorescent chemosensor for the detection of Pi in complicated environment, a **FP**-Fe^{3+} HPEES solution was also treated with Pi in the presence of different anions and polyphosphate species. As shown in Fig. 5, all of the chosen competitive anions showed minor influence on the fluorescence detection of Pi, suggesting that **FP**-Fe^{3+} is a Pi-specific fluorescence chemosensor even in the presence of competing anions.

To further understand the Fe^{3+} displacement approach, fluorescence emission changes of **FP**-Fe^{3+} in the absence and presence of different concentrations of Pi were also investigated. As shown in Fig. 6, upon addition of Pi into **FP**-Fe^{3+} solution, the fluorescence intensity increased gradually and reached saturation when 30 equiv. of Pi was added, which is

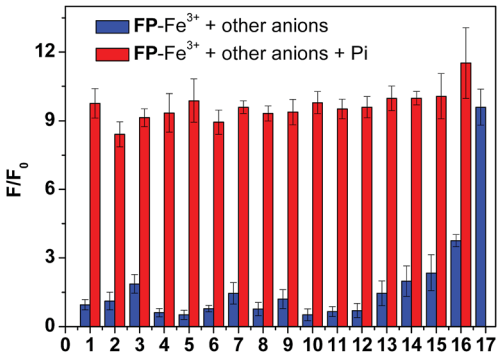

Fig. 5 Normalized fluorescence responses of FP-Fe^{3+} (10 μM) in HEPES (THF : H_2O = 3 : 7, 20 mM, pH = 7.4) in the presence of various analytes (3 × 10^{-4} M): (1) HCO_3^-, (2) F^-, (3) S^{2-}, (4) SCN^-, (5) Br^-, (6) AcO^-, (7) OH^-, (8) NO_2^-, (9) HSO_4^-, (10) Cl^-, (11) CO_3^{2-}, (12) SO_4^{2-}, (13) AMP, (14) ADP, (15) ATP, (16) PPi, (17) Pi. The intensities were recorded at 515 nm, excitation at 430 nm.

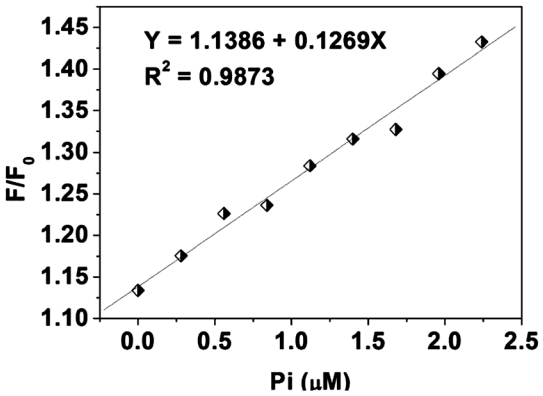

Fig. 7 The linear responses of FP (3 μM) *versus* low concentration Pi (0–2.5 μM) at 515 nm in HEPES aqueous buffer (THF : H_2O = 3 : 7, 20 mM, pH = 7.4). Excitation was performed at 430 nm.

essentially identical with the emission wavelength of free **FP**, indicating that the decomplexing of Fe^{3+} by Pi. The dose-dependent fluorescence enhancement showed a good linearity that can be expressed as $F/F_0 = 0.127[Pi] + 1.139$ ($R^2 = 0.987$) (Fig. 7). The detection limit for Pi anions, calculated according to the reported method defined by IUPAC,[16] is 3.00 × 10^{-7} M, demonstrating that **FP**-Fe^{3+} has a remarkably high sensitivity for the fluorescence sensing of Pi in aqueous solutions. Furthermore, the fast fluorescence responses of **FP**-Fe^{3+} towards Pi was also confirmed by the addition of Pi (3 × 10^{-4} M) to the solution of **FP**-Fe^{3+} (10 μM) in HEPES buffer. As shown in Fig. S11,† upon the addition of Pi, a significant fluorescence response could be observed within 5 s, indicating that the **FP**-Fe^{3+} system could be used for the real-time detection of Pi.

UV-vis absorption spectrum studies of FP-Fe^{3+} ensemble with various anions and nucleotides

Changes of UV-vis spectra were also examined by the addition of increasing concentration of Pi to the solution of **FP**-Fe^{3+} in HEPES buffer. As shown in Fig. 8. The absorption band at 480 nm decreased by the addition of 3 × 10^{-4} M Pi to the **FP**-Fe^{3+} solution. The final absorption spectrum was in agreement with the free chemosensor **FP** at identical condition, which corroborated the results of the decomplexing of Fe^{3+} in the presence of Pi. However, in the presence of other physiological and environmental important anions, such as Ac^-, Br^-, Cl^-, F^-, SCN^-, HSO_4^-, NO_2^-, OH^-, HCO_3^-, CO_3^{2-}, SO_4^{2-}, S^{2-}, and adenosine phosphate series, such as AMP, ADP, ATP, no obvious changes on absorption spectra was observed (Fig. 9), suggesting the high selectivity of **FP**-Fe^{3+} towards Pi.

Reversibility of the sensing system

The capability of reversible detection of Pi was examined by the fluorescence titration analysis. As shown in Fig. S12,† "ON–OFF–ON" fluorescence changes were observed by the alternative additions of Fe^{3+} and Pi to the solution of **FP**. And the reversible response of fluorescence intensity can be repeated more than 3 times by the modulation of Fe^{3+}/Pi addition, indicating that **FP** can be developed as a reversible fluorescence ON–OFF–ON chemosensor for Pi.

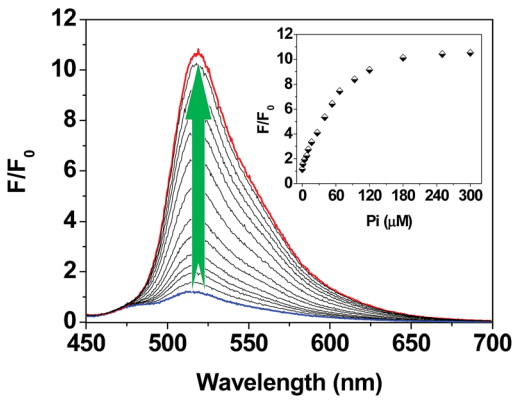

Fig. 6 Normalized fluorescence spectra of FP-Fe^{3+} (10 μM) in HEPES aqueous buffer (THF : H_2O = 3 : 7, 20 mM, pH = 7.4) in the presence of different amounts of Pi (0–3 × 10^{-4} M). Excitation was performed at 430 nm.

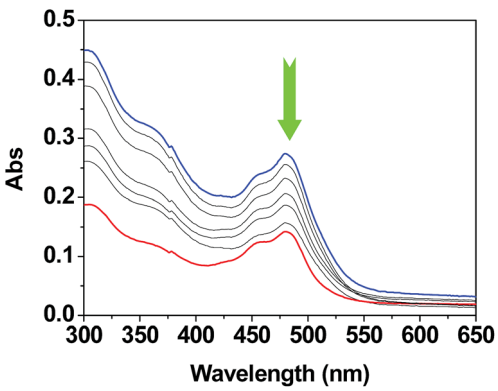

Fig. 8 UV-vis absorption spectra of FP-Fe^{3+} (10 μM) in HEPES aqueous buffer (THF : H_2O = 3 : 7, 20 mM, pH = 7.4) in the presence of different amounts of Pi (0–3 × 10^{-4} M).

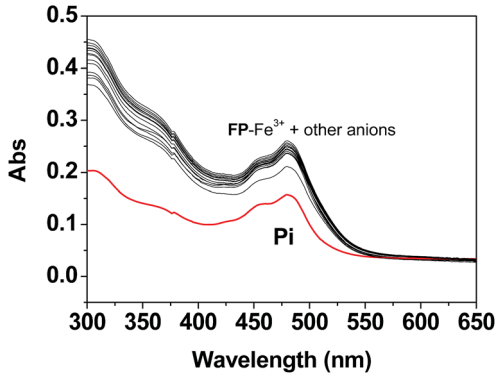

Fig. 9 Absorption spectra of **FP**-Fe^{3+} (10 μM) in HEPES aqueous buffer (THF : H_2O = 3 : 7, 20 mM, pH = 7.4) in the presence of all kinds of analytes (3 × 10^{-4} M): (1) Ac^-, (2) Br^-, (3) Cl^-, (4) F^-, (5) SCN^-, (6) HSO_4^-, (7) NO_2^-, (8) OH^-, (9) HCO_3^-, (10) CO_3^{2-}, (11) SO_4^{2-}, (12) S^{2-}, (13) AMP, (14) ADP, (15) ATP, (16) PPi, (17) Pi.

MTT assay

The cytotoxicity of **FP** toward the breast carcinoma cell line, MDA-MB-231, and human neuronal glioblastoma cell line, U-343 MGa was investigated by the reduction activity of the methyl thiazolyl tetrazolium (MTT [3-(4,5-dimethylthiazol-2-yl)-2,5-diphenyltetrazolium bromide]) assay.[20] As shown in Fig. 10, following incubation of **FP** (2–15 μM) with MDA-MB-231 for 24 h at 37 °C, no significant change in the proliferation of MDA-MB-231 cells was observed. Even after incubation with 15 μM **FP** for 24 h, the cellular viability remained above 85%, indicating that **FP** is biocompatible and suitable for fluorescence imaging in living cells. This result was also supported by the measurement of cytotoxicity in U-343 MGa cells. In the presence of **FP** with concentrations of 2–15 μM, the cellular viability was estimated to be greater than 88% after incubation for 24 h. The results revealed that **FP** is low cytotoxicity both at low and high concentration and will not kill the MDA-MB-231 and U-343 MGa cells being probed.

Confocal fluorescence imaging in live cells

Having demonstrated the high biocompatibility of **FP**, we next established the ability of **FP** to track Fe^{3+} and its **FP**-Fe^{3+} ensemble to detect Pi level in live MDA-MB-231 and U-343 MGa cells. Prior to the living cells imaging, the lipophilicity which is critical for the cellular membrane permeability of **FP** was examined by using the partition coefficient (log $P_{o/w}$) between 1-octanol and water. We confirmed that the log *P* value of **FP** was 2.37. Given that the log *P* values of fluorescence chemosensors that are known to have good cellular membrane permeability are within the range of 0–5,[21] our data suggested that **FP** is able to penetrate the cells.

The cells were incubated with a 1 μM FP in HEPES buffer for 30 min at 37 °C in a CO_2 incubator (95% relative humidity, 5% CO_2). After washed with HEPES for three times, cells were treated with 10 μM Fe^{3+} for another 20 min, followed by the incubation with 30 μM Pi for 20 min. Fig. 11 and S13† represented the results of confocal fluorescence imaging of Fe^{3+} and Pi in live MDA-MB-231 and U-343 MGa cells, respectively. As expected, both MDA-MB-231 and U-343 MGa cells exhibited bright green fluorescence after incubation with **FP** (1 μM) for 30 min (Fig. 11A and S13A, ESI†). By contrast, when **FP** deposited MDA-MB-231 and U-343 MGa cells were incubated with 10 μM Fe^{3+} for 20 min, no fluorescence was observed in both cell lines (Fig. 11B and S13B, ESI†). It is well known that the Fe^{3+} could be taken up into the live cells by diffusion through porins, and transport by transferrin and lactoferrin.[22] So, we conclude the fluorescence quenching was because of the complexation of **FP** with Fe^{3+} in the live cells. Moreover, a remarkable fluorescence enhancement was recorded when the cells were further treated with 30 μM Pi for another 20 min (Fig. 11C and S13C, ESI†), indicating that Pi penetrate live cell membrane through a sodium-dependent transporter and where it interacts with **FP**-Fe^{3+} leading to intense fluorescence emission.[23] The results suggested that **FP** is cell membrane permeable and can be employed for sensing of Fe^{3+} and its *in situ* generated **FP**-Fe^{3+} can be employed to image Pi in living cells. To the best of our knowledge, this is the first example of Fe^{3+} complexes-based displacement approach for design of the fluorescence chemosensor for Pi detection in living cells.

Quantitative **FP** deposition of MDA-MB-231 cells and its fluorescence "ON–OFF–ON" response in living cells were

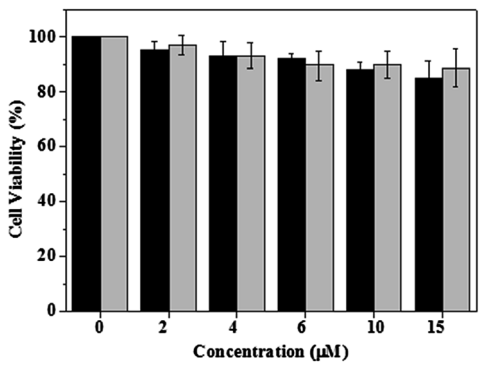

Fig. 10 Cell viability values (%) estimated by MTT proliferation test *versus* incubation concentrations. MDA-MB-231 (black bars) and U-343 MGa (gray bars) cells were incubated in the **FP** containing culture medium at 37 °C in a 5% CO_2 incubator for 24 h.

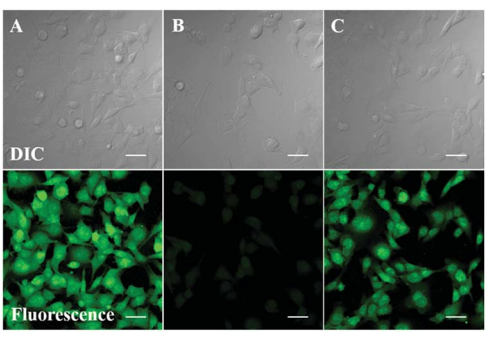

Fig. 11 Confocal bright-field (top), and fluorescence (bottom) imaging of Fe^{3+} and Pi in living MDA-MB-231 cells. (A) Cells stained with **FP** (1 μM) at 37 °C in a 5% CO_2 incubator for 30 min, (B) and treated with Fe^{3+} (10 μM) for 20 min, (C) then the cells incubated with Pi (30 μM) for another 20 min. Scale bar = 40 μm.

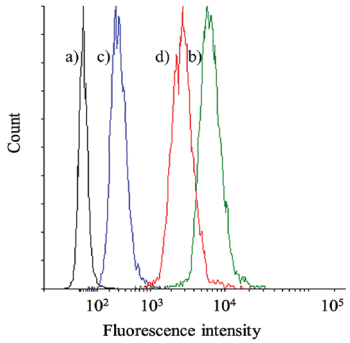

Fig. 12 Flow cytometry analysis of MDA-MB-231 cells stained with **FP** and its fluorescent response to Fe^{3+} and Pi. (a) Control group, MDA-MB-231 cells only, (b) cells stained with **FP** (1 μM) for 30 min, (c) further treated with 10 μM Fe^{3+} ions for another 20 min, (d) and then incubated with Pi (30 μM) for another 20 min.

conducted through the flow cytometer by measuring the fluorescence intensity of 10 000 cells from each population.[24] Fig. 12 represent the shift of fluorescence signal measured from live MDA-MB-231 cells stained with **FP**, treated with Fe^{3+}, and further incubated with Pi. We compared the different fluorescence intensity based on the mean fluorescence intensity (MFI) of the cell population. The MDA-MB-231 cells only (control group) displayed negligible background fluorescence (MFI: 24.79). While the fluorescence intensity of cells incubated with 1 μM **FP** for 30 min was increased dramatically (MFI: 7139.36). The treatment of cells with 10 μM Fe^{3+} for 20 min led to the significant quenching of intracellular fluorescence (MFI: 335.13). However, the recovery of the intracellular fluorescence intensity was recorded when the cells were further incubated with 30 μM Pi for another 20 min (MFI: 3057.14).

The utility of **FP**-Fe^{3+} ensembles for fluorescence imaging of Pi was further evaluated in live MDA-MB-231 and U-343 MGa cells. As shown in Fig. 13A and S14A,† staining of both MDA-MB-231 and U-343 MGa cells with 1 μM **FP**-Fe^{3+} provide no significant fluorescence. In Fig. 13B and S14B,† the cells pre-

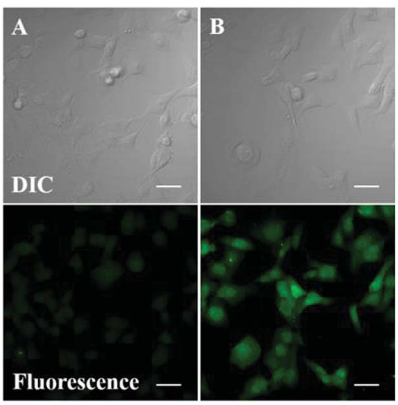

Fig. 13 Confocal bright-field (top), and fluorescence (bottom) imaging of Pi in living MDA-MB-231 cells. (A) Cells stained with **FP**-Fe^{3+} (1 μM) at 37 °C in a 5% CO_2 incubator for 30 min, (B) MDA-MB-231 cells treated with 100 μM Pi and then incubated with **FP**-Fe^{3+} (1 μM) for 30 min. Scale bar = 40 μm.

treated with 100 μM Pi for 2 h, washed with HEPES for three time to remove the remaining Pi and further incubated with 1 μM **FP**-Fe^{3+} for 30 min. The resulting bright fluorescence images in both MDA-MB-231 and U-343 MGa cells corroborated that **FP**-Fe^{3+} is able to display a fluorescence turn-ON response to Pi in the living cells.

Conclusions

We have developed a new Fe^{3+} complex, **FP**-Fe^{3+}, as the displacement strategy-based fluorescence chemosensor for Pi detection in aqueous and even in single intact cells. The specific binding of Fe^{3+} and **FP** led to 94% of fluorescence intensity quenching through a 1 : 1 complex formation. The formed nonfluorescent Fe^{3+} complex showed highly selective and sensitive to fluorescence sensing of Pi in aqueous solution through a displacement process. Compare to the currently reported chemosensors for Pi, the new chemosensor has several distinct advantages, including visible-light excitation and emission wavelengths, excellent fluorescent response with high specificity and sensitivity, and widely available pH range. Moreover, the measurements on the partition coefficient and cytotoxicity demonstrated that the good cell membrane penetration and biocompatibility of **FP**. Confocal microscopy imaging in MDA-MB-231 and U-343 MGa cells suggested that **FP** can be potentially used as a powerful tool for the imaging of Pi in live cells. In addition, we showed that **FP**-Fe^{3+} could be used to quantitative monitor intracellular Pi by flow cytometry analysis in a rapid, sensitive, and quantitative fashion. In summary, the success of this chemosensor not only provided a new method for the Pi detection in aqueous solution and living system, but also helps to extend the development of fluorescent chemosensors for other anions.

Experimental section

Materials and instruments

All reagents and solvents were of AR grade and used without further purification unless otherwise noted. Fluorescein, hydrazine hydrate and 2-aminopyridine were purchased from Sinopharm Chemical Reagent Co., Ltd. (China); MTT (3-(4,5-dimethylthiazol-2-yl)-2,5-diphenyltetrazolium bromide), Roswell Park Memorial Institute's Medium (RPMI-1640), Dulbecco's Modified Eagle Medium (DMEM), fetal bovine serum (FBS), L-glutamine, penicillin, and streptomycin sulphate were purchased from Life Technologies (Australia). ^{1}H-NMR and ^{13}C-NMR spectra were recorded with a AVANCE 500 MHz spectrometer (BRUKER) with chemical shifts reported as ppm (in DMSO, TMS as internal standard). API mass spectra were recorded on a HP1100LC/MSD spectrometer. The elemental analyses of C, H, N and O were performed on a Vario EL III elemental analyzer. Fluorescence spectra were determined with LS 55 luminescence spectrometer (Perkin Elmer, USA). The absorption spectra were measured with a Lambda 900 UV/VIS/NIR spectrophotometer (Perkin Elmer, USA). Fluorescent live cell images were acquired on an Olympus Fluoview FV 1000 IX81 inverted confocal laser-scanning microscope equipped

with 405, 473, 559 and 635 nm laser diodes. All of the images were analysed by using Image J software version 1.44p. Flow cytometry analysis was recorded on a BD FACSAria II flow cytometer with a 488 nm laser. The data were analysed with Flowing software.

General procedures of spectra detection

Fresh stock solution of metal ions (nitrate salts, 20 mM) and anions (as sodium salts, 20 mM) in H_2O were prepared for further experiments. Stock solutions of **FP** was prepared in HEPES aqueous buffer (THF : H_2O = 3 : 7, 20 mM, pH = 7.4). Before spectroscopic measurements, the solution was freshly prepared by diluting the high concentration stock solution to corresponding solution (10 μM). Excitation wavelength for **FP** and its complex **FP**-Fe^{3+} was performed at 430 nm. The excitation and emission slit widths were of 5 nm and 10 nm, respectively. Each time a 3 mL solution of chemosensor was filled in a quartz cell of 1 cm optical path length, and different stock solutions of cations and anions were added into the quartz cell gradually by using a micro-syringe.

Association constant calculation

Generally, for the formation of 1 : 1 complexation species formed by the chemosensor compound and the guest cations, the Benesi–Hildebrand equation used is as follow:[25]

$$\frac{1}{F_0 - F} = \frac{1}{K_a(F_0 - F_{min})[Fe^{3+}]} + \frac{1}{F_0 - F_{min}}$$

where F and F_0 represent the fluorescence emission of **FP** in the presence and absence of Fe^{3+}, respectively, F_{min} is the saturated emission of **FP** in the presence of excess amount of Fe^{3+}; $[Fe^{3+}]$ is the concentration of Fe^{3+} ion added, and K_a is the binding constant.

Synthesis and characterization of the fluorescent chemosensor

4-Fluoresceincarboxaldehyde was prepared according to a reported procedure with 30% yield.[26] To a solution of 4-fluoresceincarboxaldehyde (0.360 g, 1 mmol) in 20 mL methanol, 2-aminopyridine (0.103 g, 1.1 mmol) in 10 mL methanol was added at room temperature. The stirred reaction mixture was heated to reflux for 6 h to yield a yellow precipitate. After cooling to room temperature, the precipitate was washed with methanol and dried under vacuum to obtain **FP** in 80% yield. ^{1}H NMR (*d*-DMSO, 500 MHz), δ (ppm) 14.86 (s, 1H), 10.24 (s, 1H), 10.09 (s, 1H), 8.65 (s, 1H), 8.03–7.98 (2H, dd), 7.81 (t, J = 7.5 Hz, 1H), 7.74 (t, J = 7.5 Hz, 1H), 7.60 (d, J = 5.0 Hz, 1H), 7.45 (d, J = 5.0 Hz, 1H), 7.35 (d, J = 10.0 Hz, 1H), 6.86–6.81 (m, 2H), 6.71 (d, J = 10.0 Hz, 1H), 6.62 (s, 2H). ^{13}C NMR (*d*-DMSO, 125 Hz), δ (ppm) 168.0, 164.7, 159.0, 157.6, 155.4, 151.7, 150.5, 148.7, 138.7, 133.5, 128.5, 122.8, 119.0, 112.8, 107.7, 105.8, 101.9, 81.7. ES-API (positive mode, m/z) calcd for $C_{26}H_{16}N_2O_5$: 436.11. Found: 437.2 (**FP** + H^+). Anal. calcd for: C, 71.56; H, 3.70; N, 6.42. Found: C, 71.34; H, 3.89; N, 6.47.

Evaluation of partition coefficient

1-Octanol/water partition coefficients ($P_{o/w}$) for **FP** was obtained using the 'shake-flask' method.[20] Briefly, **FP** was dissolved in water (1 mM), and was diluted with 2 mL 1-octanol-saturated PBS (pH 7.4). Then, 2 mL of water-saturated 1-octanol solution was added into the solution with continuous stirring. The mixture was stirred at R. T. for another 2 h before examining the concentrations of the complexes in water phase before and after partitioning by absorbance measurements. The $P_{o/w}$ of **FP** was calculated according to the following formula: $P_{o/w} = (C_{before} - C_{after})/C_{after}$. The experiment was repeated three times.

Cell line and cell culture

The breast adenocarcinoma cell line, MDA-MB-231, was obtained from American Type Culture Collection (ATCC® HTB-26™). MDA-MB-231 cells were maintained in RPMI-1640 supplemented with 10% (v/v) fetal bovine serum (FBS), L-glutamine (2 mM), penicillin (100 μg mL^{-1}), streptomycin sulphate (100 μg mL^{-1}) and HEPPS buffer. Human neuronal glioblastoma cell line, U-343 MGa, was purchased from CLS Cell Lines Service GmbH, German. U-343 MGa cells were grown in DMEM supplemented with 10% (v/v) fetal bovine serum (FBS), L-glutamine (2 mM), D-glucose (4.5 g L^{-1}), sodium pyruvate (110 mg L^{-1}), penicillin (100 μg mL^{-1}), streptomycin sulphate (100 μg mL^{-1}). All of the cells were grown in a humidified 37 °C, 5% CO_2/95% air (v/v) incubator. The growth medium was changed every two days. The cells were routinely subcultured using 0.05% trypsin–EDTA solution and growth to 80% confluence prior to experiment.

MTT assay

MDA-MB-231 and U-343 MGa cells were seeded at a density of 5×10^4 cells per mL in a 96-well micro-assay culture plate and growth 24 h at 37 °C in a 5% CO_2 incubator. **FP** in fresh culture medium was added into each well with different concentrations from 2 to 15 μM. Control wells were prepared by the addition of culture medium, and wells containing culture media without cells were used as blanks. After incubation at 37 °C in a 5% CO_2 incubator for 24 h, cell culture medium was removed and cells were washed three times with PBS. Then, 100 μL, 0.5 mg mL^{-1} MTT solution in PBS was added to each well, and the cells were further incubated for 4 h. The excess MTT solution was then carefully removed from wells, and the formed formazan was dissolved in 100 μL of DMSO (dimethyl sulfoxide). The optical density of each well was then measured at a wavelength of 590 nm using a microplate reader (Bio-Rad, xMark). The following formula was used to calculate the viability of cell growth: viability (%) = (mean of absorbance value of treatment group − blank)/(mean absorbance value of control − blank) × 100.

Confocal fluorescence imaging in live cells

For live cells imaging of "ON–OFF–ON" response towards Fe^{3+} and Pi. MDA-MB-231 and U-343 MGa cells were typically seeded at a density of 5×10^4 cells per mL in a 22 mm

coverglass bottom culture dishes (ProSciTech, AU) for the confocal microscope imaging. The cells were washed with HEPES buffer for three times, and then stained with 1 M **FP** in HEPES buffer at 37 °C in a 5% CO_2 incubator. After 30 min, the cells were washed with more HEPES (3 × 2 mL per dish) to remove excess **FP**. The **FP** loaded cells were treated with 10 μM Fe^{3+} in HEPES for another 20 min, washed three times with HEPES (1 mL per well), and then further incubated with HEPES containing 30 μM Pi for 20 min. The cells were washed with HEPES for three times before subjecting to microscope imaging.

For live cell imaging of "OFF–ON" response of FP-Fe^{3+} towards Pi. MDA-MB-231 and U-343 MGa cells were incubated with 100 μM Pi in an atmosphere of 5% CO_2 and 95% air for 2 h at 37 °C. After washed with HEPES for three times, the cells were further stained with 1 μM **FP**-Fe^{3+} in HEPES buffer for another 30 min. The cells were washed with HEPES for three times before subjecting to microscope imaging.

Flow cytometry analysis

MDA-MB-231 cells (1×10^5 cells per mL) were plated into a six-chamber culture well and incubated for 24 h. The cells were washed with HEPES for three times, then stained with 1 μM **FP** in HEPES at 37 °C in a 5% CO_2 incubator for 30 min. After washed with HEPES for three times, the cells were treated with 10 μM Fe^{3+} in HEPES for another 20 min. 30 μM Pi in HEPES buffer was added to each well and then, the cells were further incubated at 37 °C for 20 min. The cells were detached from the well using 0.05% trypsin–EDTA solution and washed with PBS for three times before flow cytometry analysis. Cells incubated with RPMI-1640 for 24 h were used as the controls for all experiments.

Acknowledgements

This work is supported by the National Natural Science Foundation of China (no. 21301011) and the State Key Laboratory of Fine Chemicals (KF1305), and Macquarie University Research Fellowship Scheme (MQRF-1487520).

Notes and references

1 (*a*) S. Lee, K. K. Y. Yuen, K. A. Jolliffe and J. Yoon, *Chem. Soc. Rev.*, 2015, **44**, 1749–1762; (*b*) L. Fabbrizzi and A. Poggi, *Chem. Soc. Rev.*, 2012, **42**, 1681–1699; (*c*) P. A. Gale, N. Busschaert, C. J. E. Hayness, L. E. Karagiannidis and I. L. Kirby, *Chem. Soc. Rev.*, 2014, **43**, 205–241; (*d*) K.-C. Chang, S.-S. Sun, M. O. Odago and A. J. Lees, *Coord. Chem. Rev.*, 2015, **284**, 111–123; (*e*) F. Mancin, E. Rampazzo, P. Tecilla and U. Tonellato, *Chem.–Eur. J.*, 2006, **12**, 1844–1854; (*f*) L. E. Santos-Figueroa, M. E. Moragues, E. Climent, A. Agostini and R. Martínez-Máñez, *Chem. Soc. Rev.*, 2013, **42**, 3489–3613; (*g*) M. H. Lee, J. S. Kim and J. L. Sessler, *Chem. Soc. Rev.*, 2015, DOI: 10.1039/c4cs00280f; (*h*) L. Zhu, Z. Yuan, J. T. Simmons and K. Sreenath, *RSC Adv.*, 2014, **4**, 20398–20440; (*i*) Y. Ding, Y. Tang, W. Zhua and Y. Xie, *Chem. Soc. Rev.*, 2015, **44**, 1101–1112.

2 (*a*) E. G. Krebs and J. A. Beavo, *Annu. Rev. Biochem.*, 1979, **48**, 923–959; (*b*) L. Rothfield and A. Finkelstein, *Annu. Rev. Biochem.*, 1968, **37**, 463–496; (*c*) W. P. Jencks, *Annu. Rev. Biochem.*, 1997, **66**, 1–18; (*d*) N. M. Hansen, R. Felix, S. Bisaz and H. Fleisch, *Biochim. Biophys. Acta*, 1976, **451**, 549–559; (*e*) G. R. Beck Jr, E. Moran and N. Knecht, *Exp. Cell Res.*, 2003, **288**, 288–300.

3 (*a*) H. Jin, S.-K. Hwang, J.-T. Kwon, Y.-S. Lee, G.-H. An, K.-H. Lee, A.-C. Prats, D. Morello, G. R. Beck Jr and H. Cho, *J. Nutr. Biochem.*, 2008, **19**, 16–25; (*b*) C. F. Dick, A. L. A. Dos-santos and J. R. Meyer-Fernandes, *Biochim. Biophys. Acta*, 2014, **1840**, 2123–2127; (*c*) Y. Tasaki, Y. Kamiya, A. Azwan, T. Hara and T. Joh, *Biosci., Biotechnol., Biochem.*, 2002, **66**, 790–800.

4 (*a*) E. Takeda, H. Yamamoto, K. Nashiki, T. Sato, H. Arai and Y. Taketani, *J. Cell. Mol. Med.*, 2004, **8**, 191–200; (*b*) C. Auesukaree, T. Homma, H. Tochio, M. Shirakawa, Y. Kaneko and S. Harashima, *J. Biol. Chem.*, 2004, **279**, 17289–17294; (*c*) J. P. Knochel, *Arch. Intern. Med.*, 1977, **137**, 203–220; (*d*) A. Shaikh, T. Berndt and R. Kumar, *Pediatr. Nephrol.*, 2008, **23**, 1203–1210.

5 (*a*) N. Ahmed, V. Suresh, B. Shirinfar, I. Geronimo, A. Bist, I. Hwang and K. S. Kim, *Org. Biomol. Chem.*, 2012, **10**, 2094–2100; (*b*) V. V. S. Mummidivarapu, V. K. Hinge and C. P. Rao, *Dalton Trans.*, 2015, **44**, 1130–1141; (*c*) S. Berchmans, T. B. Issa and P. Singh, *Anal. Chim. Acta*, 2012, **729**, 7–20; (*d*) G. Zhang, B. Lua, Y. Wen, L. Lu and J. Xua, *Sens. Actuators, B*, 2012, **171**, 786–794; (*e*) G. Saikia and P. K. Iyer, *Macromolecules*, 2011, **44**, 3753–3758; (*f*) J. Wang and C.-S. Ha, *Analyst*, 2010, **135**, 1214–1218; (*g*) S. Mizukami, T. Nagano, Y. Urano, A. Odani and K. Kikuchi, *J. Am. Chem. Soc.*, 2002, **124**, 3920–3925; (*h*) H. N. Lee, K. M. K. Swamy, S. K. Kim, J.-Y. Kwon, Y. Kim, S.-J. Kim, Y. J. Yoon and J. Yoon, *Org. Lett.*, 2007, **9**, 243–246; (*i*) J. Hatai, S. Pal and S. Bandyopadhyay, *Tetrahedron Lett.*, 2012, **53**, 4357–4360; (*j*) A. K. Dwivedi, G. Saikia and P. K. Iyer, *J. Mater. Chem.*, 2011, **21**, 2502–2507; (*k*) B. P. Morgan, S. He and R. C. Smith, *Inorg. Chem.*, 2007, **46**, 9262–9266; (*l*) B.-K. Son, M. Akishita, K. Iijima, S. Ogawa, T. Arai, H. Ishii, K. Maemura, H. Aburatani, M. Eto and Y. Ouchi, *J. Mol. Cell. Cardiol.*, 2013, **56**, 72–80; (*m*) J. Liu, K. Wu, X. Li, Y. Han and M. Xia, *RSC. Adv.*, 2013, **3**, 8924–8928; (*n*) P. Saluja, N. Kaur, N. Singh and D. O. Jang, *Tetrahedron Lett.*, 2012, **53**, 3292–3295; (*o*) L. E. Guo, J. F. Zhang, X. Y. Liu, L. M. Zhang, H. L. Zhang, J. H. Chen, X. G. Xie, Y. Zhou, K. Luo and J. Yoon, *Anal. Chem.*, 2015, **87**, 1196–1201; (*p*) E. Kittiloespaisan, I. Takashima, W. Kiatpathomchai, J. Wongkongkatep and A. Ojida, *Chem. Commun.*, 2014, **50**, 2126–2129.

6 (*a*) Q.-Y. Cao, T. Pradhan, S. Kim and J. S. Kim, *Org. Lett.*, 2011, **13**, 4386–4389; (*b*) C. M. G. Santos, E. M. Boyle, S. D. Solis, P. E. Krugerc and T. Gunnlaugsson, *Chem. Commun.*, 2011, **47**, 12176–12178; (*c*) K. Ghosh, S. S. Ali and S. Joardar, *Tetrahedron Lett.*, 2012, **53**, 2054–2058.

7 J. Wu, Z. Ye, G. Wang, D. Jin, J. Yuan, Y. Guan and J. Piper, *J. Mater. Chem.*, 2009, **19**, 1258–1260.
8 (*a*) D. Karak, S. Das, S. Lohar, A. Banerjee, A. Sahana, I. Hauli, S. K. Mukhopadhyay, D. A. Safin, M. G. Babashkina, M. Bolte, Y. Garcia and D. Das, *Dalton Trans.*, 2013, **42**, 6708–6715; (*b*) L. Xu, Y. Xu, W. Zhu, B. Zeng, C. Yang, B. Wu and X. Qian, *Org. Biomol. Chem.*, 2011, **9**, 8284–8287; (*c*) J.-T. Hou, K. Li, K.-K. Yu, M.-Y. Wu and X.-Q. Yu, *Org. Biomol. Chem.*, 2013, **11**, 717–720; (*d*) C. Kar, M. D. Adhikari, A. Ramesh and G. Das, *Inorg. Chem.*, 2013, **52**, 743–752; (*e*) X. Cao, W. Lin and L. He, *Org. Lett.*, 2011, **13**, 4716–4719; (*f*) I. Takashima, M. Kinoshita, R. Kawagoe, S. Nakagawa, M. Sugimoto, I. Hamachi and A. Ojida, *Chem.–Eur. J.*, 2014, **20**, 2184–2192.
9 X. Lou, D. Ou, Q. Li and Z. Li, *Chem. Commun.*, 2012, **48**, 8462–8477.
10 (*a*) Q. Meng, Y. Shi, C. Wang, H. Jia, X. Gao, R. Zhang, Y. Wang and Z. Zhang, *Org. Biomol. Chem.*, 2015, **13**, 2198–2926; (*b*) R. Zhang, X. Yu, Y. Yin, Z. Ye, G. Wang and J. Yuan, *Anal. Chim. Acta*, 2011, **691**, 83–89.
11 (*a*) S. K. Sahoo, D. Sharma, R. K. Bera, G. Crisponi and J. F. Callan, *Chem. Soc. Rev.*, 2012, **41**, 7195–7227; (*b*) J. Han, J. Jose, E. Mei and K. Burgess, *Angew. Chem.*, 2007, **46**, 1684–1687; (*c*) S. Fujishima, R. Yasui, T. Miki, A. Ojida and I. Hamachi, *J. Am. Chem. Soc.*, 2012, **134**, 3961–3964.
12 (*a*) M. Kumar, R. Kumar and V. Bhalla, *Org. Lett.*, 2011, **12**, 366–369; (*b*) G. E. Tumambac, C. M. Rosencrance and C. Wolf, *Tetrahedron*, 2004, **60**, 11293–11297.
13 T.-B. Wei, P. Zhang, B.-B. Shi, P. Chen, Q. Lin, J. Liu and Y.-M. Zhang, *Dyes Pigm.*, 2013, **97**, 297–302.
14 (*a*) R. Zhang, B. Son, Z. Dai, Z. Ye, Y. Xiao, Y. Liu and J. Yuan, *Biosens. Bioelectron.*, 2013, **50**, 1–7; (*b*) C.-F. Chow, F.-W. Gong and C.-B. Gong, *Analyst*, 2014, **139**, 4532–4537.
15 R. Koteeswari, P. Ashokkumar, E. J. P. Malar, V. T. Ramakrishnan and P. Ramamurthy, *Chem. Commun.*, 2011, **47**, 7695–7697.
16 (*a*) J. Mocak, A. M. Bond, S. Mitchell and G. Scollary, *Pure Appl. Chem.*, 1997, **69**, 297–302; (*b*) V. Thomsen, D. Schatzlein and D. Mercuro, *Spectroscopy*, 2003, **18**, 112–118.
17 J. A. Dean, *Langès Handbook of Chemistry*, McGraw-Hill, New York, 15th edn, 1999.
18 (*a*) M. Kumar, R. Kumar, V. Bhalla, P. R. Sharma, T. Kaur and Y. Qurishi, *Dalton Trans.*, 2012, **41**, 408–412; (*b*) A. Goel, S. Umar, P. Nag, A. Sharma, L. Kumar, Shamsuzzama, Z. Hossain, J. R. Gayen and A. Nazir, *Chem. Commun.*, 2015, **51**, 5001–5004.
19 S. Patra, R. Lo, A. Chakraborty, R. Gunupuru, D. Maity, B. Ganguly and P. Paul, *Polyhedron*, 2013, **50**, 592–601.
20 (*a*) C. Li, M. Yu, Y. Sun, Y. Wu, C. Huang and F. Li, *J. Am. Chem. Soc.*, 2011, **133**, 11231–11239; (*b*) X. Wang, Y. Xia, Y. Liu, W. Qi, Q. Sun, Q. Zhao and B. Tang, *Chem.–Eur. J.*, 2012, **18**, 7189–7195; (*c*) C. Huang, T. Jia, M. Tang, Q. Yin, W. Zhu, C. Zhang, Y. Yang, N. Jia, Y. Xu and X. Qian, *J. Am. Chem. Soc.*, 2014, **136**, 14237–14244.
21 (*a*) R. W. Horobin, J. C. Stockert and F. Rashid-Doubell, *Histochem. Cell Biol.*, 2006, **126**, 165–172; (*b*) H. Komatsu, K. Yoshihara, H. Yamada, Y. Kimura, A. Son, S. Nishimoto and K. Tanabe, *Chem.–Eur. J.*, 2013, **19**, 1971–1977.
22 (*a*) D. M. Templeton, *Molecular and cellular iron transport*, Marcel Dekker, New York, Illustrated edn, 2002; (*b*) E. L. Mackenzie, K. Iwasaki and Y. Tsuji, *Antioxid. Redox Signaling*, 2008, **10**, 997–1014.
23 M. R. Hammerman, *Am. J. Physiol.*, 1986, **251**, F385–F398.
24 H. Yu, Y. Xiao and L. Jin, *J. Am. Chem. Soc.*, 2012, **134**, 17486–17489.
25 B. Valeur, *Molecular Fluorescence: Principles and Applications*, Wiley-VCH, Weinheim, 2002.
26 H. F. Blum and C. R. Spealman, *J. Phys. Chem.*, 1932, **37**, 1123–1133.